ACS Sustainable Chemistry & Engineering

Article

Phosphoryl-Ligand Adducts of Rare Earth-TriNOx Complexes: Systematic Studies and Implications for Separations Chemistry

Thibault Cheisson, Bren E. Cole, Brian C. Manor, Patrick J. Carroll, and Eric J. Schelter

ACS Sustainable Chem. Eng., **Just Accepted Manuscript** • DOI: 10.1021/acssuschemeng.8b05638 • Publication Date (Web): 18 Jan 2019

ACS Publications

is published by the American Chemical Society. 1155 Sixteenth Street N.W., Washington, DC 20036

Phosphoryl-Ligand Adducts of Rare Earth-TriNOx Complexes: Systematic Studies and Implications for Separations Chemistry

Thibault Cheisson, Bren E. Cole, Brian C. Manor, Patrick J. Carroll, and Eric J. Schelter∗

∗Corresponding author: schelter@sas.upenn.edu

P. Roy and Diana Vagelos Laboratories, Department of Chemistry, University of Pennsylvania, 231 S. 34th St., Philadelphia, PA 19104, USA.

KEYWORDS. Separations, Rare Earths, Lanthanides, Leaching, Recycling, Coordination Chemistry

ABSTRACT

Phosphoryl ligands of the general formula $O=PR_3$ (R= Me, OMe, Et, ^{n}Bu, Ph, ^{i}Pr, NMe_2) were coordinated to [Nd(TriNOx)] ($TriNOx^{3-}$ = [(2-^{t}BuNO)$C_6H_4CH_2]_3N)^{3-}$) and the resulting complexes were characterized. Solution equilibrium constants for each complex were determined, demonstrating a large range for phosphoryl ligands Lewis basicity. Thermogravimetric analyses provided evidence for the qualitative thermodynamic preference of phosphoryl ligands for [Nd(TriNOx)] over the dysprosium analogue. These findings were exploited for the separation of binary mixtures of neodymium/dysprosium and lanthanum/neodymium. Implementation of phosphoryl ligands in the TriNOx separation system expands its scope and demonstrates a fundamentally different mode for separating rare-earth cations based on adducts with neutral donors.

INTRODUCTION

Urban mining of spent materials has been proposed as a sustainable approach to exploit secondary sources of critical elements. Such a strategy should allow for reduction of the environmental impact of mining while

diminishing the strategic dependence on primary producers.[1] In fact, some metallurgical industries have already transitioned to a larger incorporation of recycled scraps into their supply chains. For example, 36 % of gold, 25 % of silver and 35 % of copper are obtained from recycling today.[1] On the other hand, rare earth elements (RE) have become ubiquitous in modern technologies but, as recently as 2011, only 1% of were recovered from end of life materials.[2-4] As summarized in Table 1, RE production from natural ores has detrimental impacts on the environment and the surrounding populations.[5-7] Therefore, there is a clear need and opportunity to develop a circular RE economy through recycling,[4, 8] as determined by several life-cycle assessments.[9-11]

Table 1. Selected data for the production of 1 kg of Nd_2O_3 from Bayan Obo (China) adapted and averaged from references.[5, 7, 9]

Item	Raw ore	Global warming	Acidification	Eutrophication	Human toxicity	Radioactive dust
Units	kg	kg CO_2 eq	kg SO_2 eq	kg PO_4 eq	kg 1,4-DCB eq	g

Value	330	58	0.5	0.1	69	20

Flowsheets have been proposed for the preconcentration of REs from scraps,[12-13] however REs are generally recovered as variable mixtures of the elements, which prevents their direct reintroduction into the supply chain. Refinement of these recovered RE blends is currently achieved by solvent extraction,[14] an effective but solvent- and energy-consuming method.[5-6]

In recent years, progress has been made in developing alternative methods for targeted RE separations such as ionic liquid-based separations systems,[15-17] selective crystallization[18-21] or photochemical reduction.[22-23] Immobilized extractants such as bacteria[24-26] or functionalized materials have also shown promising capabilities.[27-32] Recovery of RE from end of life materials actually provides simplified mixtures of REs with relative ratios very different from the natural ores. Such mixtures provide an opportunity for simpler operations than those used in a solvent extraction separation plant. In this contribution, we focus on non-adjacent pairs of REs of technological relevance, such as Nd/Dy

found in hard permanent magnets or La/Nd found at the anode of nickel metal-hydride (NiMH) batteries.[13, 33-34]

Our group recently demonstrated the separation of early/late RE combinations using the self-association/complexation properties of RE-compounds bearing a tripodal anionic ligand, $([(2\text{-}^{t}BuNO)C_6H_4CH_2]_3N)^{3-}$ ($TriNOx^{3-}$).[35-37] The chelation of three hard, anionic donors to a RE center led to the formation of complexes bearing a size-sensitive molecular aperture that was responsible for large differences in the self-association equilibria (K_{dimer}, see Scheme 1) based upon small changes in ionic radii across the lanthanide series. Solubility differences between the resulting early RE dimer ($[(RE)TriNOx]_2$, RE = La-Eu) and late RE monomer ([(RE)TriNOx(THF)], RE = Y, Gd-Lu) complexes afforded good separation factors by a simple leaching in benzene ($S_{Nd/Dy}$ = 303) or toluene ($S_{Nd/Dy}$ = 30).[37] Employing the ability of $TriNOx^{3-}$ to undergo ligand-based oxidation, we also demonstrated the separation of late/late RE pairs by an electro-kinetic method.[38] In both cases, the key contributions were the elucidation of a molecular basis to achieve separation of RE pairs.

The factor responsible for the exceptional selectivity for some RE-pairs of this seminal system, namely selective self-association for early RE pairs, are also its main limitation for extension to other RE-pairs, especially for early/early or late/late combinations of REs. A simple option for adjusting the $TriNOx^{3-}$ system is the use of readily available external ancillary ligands that interact differentially with the isostructural [(RE)TriNOx(THF)] series. We hypothesized that the exceptional fine tuning of the molecular aperture observed within the [(RE)TriNOx(THF)] series could result in different binding affinities across the RE series for a given ligand, enabling separations. As well-established neutral ligands for RE cations, with easily tunable electronic and steric profiles,[39-42] we selected a library of 7 phosphoryl ligands (Chart 1, $O=PR_3$, R = Me, OMe, Et, ^{n}Bu, Ph, ^{i}Pr, NMe_2) to investigate [(RE)TriNOx] separation mediated by ancillary ligands. Coordination to [Nd(TriNOx)] and [Dy(TriNOx)] was explored by solution- and solid-state methods. Separation experiments employing phosphoryl ligands resulted in good separations factors between Nd and Dy over a single step. Moreover, implementation of phosphoryl ligands in our separation system

allow for more benign leaching solvents; while permitting the separation of early/early lanthanide mixtures, separations that were previously not possible. The current report focuses on simulated pairs of REs in idealized conditions, but, the results contribute to the development of alternatives to solvent extraction for targeted REs separations, especially for urban mining applications.

Chart 1. Library of phosphoryl ligands ($O=PR_3$) investigated in this work.

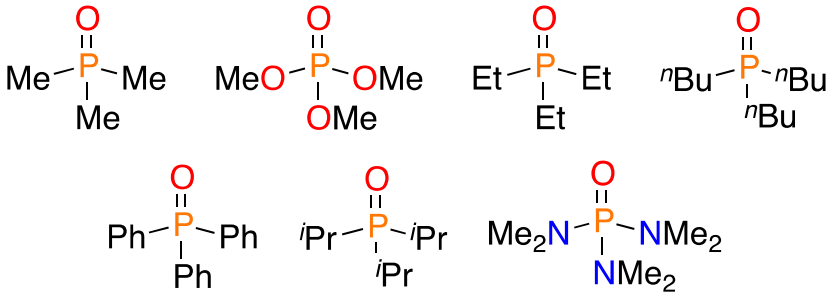

RESULTS AND DISCUSSION

Syntheses and solution behavior of complexes. The neodymium complexes **2**-**8** were synthesized from the parent THF adduct ($\mathbf{1}_{\mathbf{THF}}$) using excess of the free phosphoryl ligands (Scheme 1). Adducts **2**-**8** were isolated as crystalline

solids in fair to good yields (see Experimental Section and SI for synthetic details).

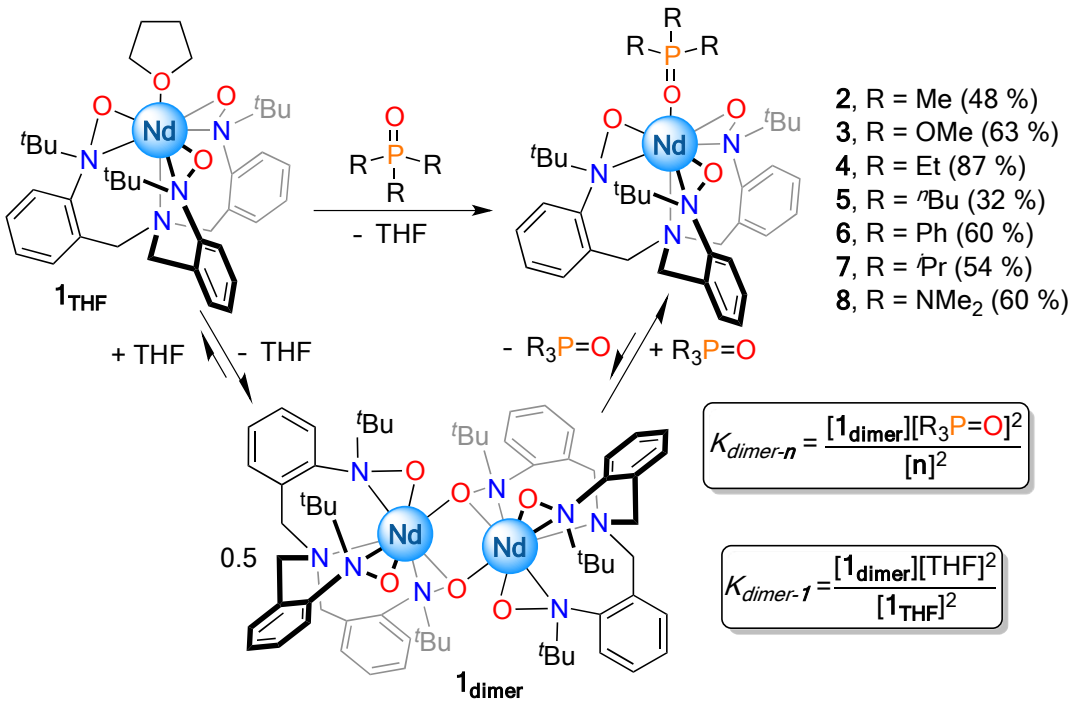

Scheme 1. Syntheses of complexes **2**-**8** and dimerization equilibrium constants $K_{dimer\text{-}n}$ (**n** = **1**-**8**).

^{1}H and ^{31}P{^{1}H} NMR spectra were recorded for compounds **2**-**8** in $CDCl_3$, demonstrating the coordination of a single equivalent of phosphoryl ligand to form the monomeric C_3-symmetric complexes **2**-**8** (see SI). As described by us previously, adducts $\mathbf{1}_{THF}$ and **2**-**8** are involved in self-association equilibria to

form the dimeric complex $\mathbf{1_{dimer}}$ (Scheme 1).[35] The equilibrium constant $K_{dimer\text{-}n}$ (n = **1**-**8**) was defined for the formation of $\mathbf{1_{dimer}}$ and measured in C_6D_6:$CDCl_3$ mixtures to afford solubility of all phosphoryl ligands (Table 2 and Figures S22-S30).

Table 2. Self-association equilibrium constants $K_{dimer\text{-}n}$ (n = **1**-**8**) for complexes **1**-**8** in C_6D_6/$CDCl_3$ mixtures.

Ligand	THF ($\mathbf{1_{THF}}$)	O=PMe$_3$ (**2**)	O=P(OMe)$_3$ (**3**)	O=PEt$_3$ (**4**)
$K_{dimer\text{-}n}$ (M)	6.3±0.6	4.5±2.3 × 10^{-3}	2.0±0.2	2.9±0.5 × 10^{-2}
Ligands	O=P^{n}Bu$_3$ (**5**)	O=PPh$_3$ (**6**)	O=P^{i}Pr$_3$ (**7**)	O=P(NMe$_2$)$_3$ (**8**)
$K_{dimer\text{-}n}$ (M)	1.1±0.1 × 10^{-2}	1.0±0.1 × 10^{-1}	6.9±2.1 × 10^{-3}	8.7±0.8 × 10^{-3}

The magnitude of the dimerization equilibria was strongly impacted by the nature of the ancillary phosphoryl ligand (Scheme 1, $K_{dimer\text{-}n}$ ranges 2.0 to 4.5 × 10^{-3} M). Several Lewis basicity and affinity scales have been described in the literature and can be compared with the values of $K_{dimer\text{-}n}$ (see Figure S31).[43] The tabulated Lewis basicity trends are reproduced for $K_{dimer\text{-}n}$: alkyl phosphine oxides and hexamethylphosphoramide (HMPA) are the strongest Lewis bases. In comparison, aromatic phosphine oxides, such as O=PPh$_3$, are

weaker Lewis bases but they are still more basic than organophosphates (*e.g.* $O=P(OMe)_3$). Finally, THF ranks as the weakest Lewis base of the series. These comparisons confirmed a clear correlation between the inherent Lewis basicity of the phosphoryl ligands and the respective dimerization constants of complexes **2**-**8**. Within the alkyl phosphine oxide ligand types, small variations of $K_{dimer\text{-}n}$ were not reproduced in the Lewis basicity and affinity scales, an observation that supports a steric contribution that is not present in usual measurements of Lewis basicity.[43]

Having established the solution behavior of neodymium adducts **1**-**8**, the coordination of phosphoryl ligands was examined for the dysprosium analogue $\mathbf{9_{THF}}$.[35] As we previously reported, the self-association of $\mathbf{9_{THF}}$ to form a dimeric analogue of $\mathbf{1_{dimer}}$ is strongly disfavored on thermodynamic grounds, as extrapolated from the self-association constants of early lanthanide analogues (La-Sm).[36] This absence of self-association was found to be the main factor responsible for the high separation factor observed between neodymium and dysprosium observed in our initial report.[35] Interestingly, over the course of the

present study, we identified the unsolvated complex $\mathbf{9_{ø}}$ (Scheme 2). This complex exhibited C_3 symmetry in $CDCl_3$ and confirmed the hypothesis that a dimeric dysprosium analogue of $\mathbf{1_{dimer}}$ would not form to a measurable degree, even in the absence of an apical, ancillary ligand.

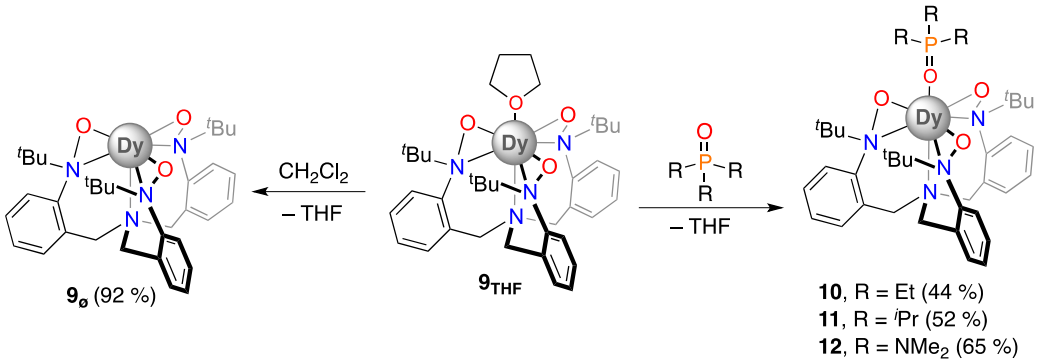

Scheme 2. Syntheses of the dysprosium complexes $\mathbf{9_{ø}}$ and **10**–**12**.

Syntheses of the dysprosium analogues of complexes **2**–**8** were attempted but, isolable and analytically pure complexes were only obtained for the phosphine oxides $O{=}PEt_3$ (**10**) and $O{=}P(^{i}Pr)_3$ (**11**) and the phosphoramidate HMPA (**12**) (Scheme 2). As expected, these complexes were determined to be C_3-symmetric in $CDCl_3$ with one equivalent of phosphoryl ligand coordinated. Because of the insolubility of $\mathbf{9_{THF}}$ and $\mathbf{9_{ø}}$ in most solvents, it was not possible

to determine meaningful binding constants for complexes **10**–**12** by NMR spectroscopy.

Solid-state crystallography. Neodymium complexes **2**–**8** and dysprosium complexes $\mathbf{9_{ø}}$, **10**–**12** were crystallized (Table S2) and characterized by X-ray diffraction crystallography. As indicated by ^{1}H NMR spectroscopy, all phosphoryl adducts were observed to contain only one equivalent of ancillary ligand. All complexes exhibited the expected coordination mode of the TriNOx^{3-} ligand observed for rare-earth cations (*e.g.* tridentate κ^2-(N,O)). As representative examples, thermal ellipsoid plots of complexes, **2**, **5**, and $\mathbf{9_{ø}}$ are depicted in Figure 1 (see Figures S32-S39 for remaining complexes).

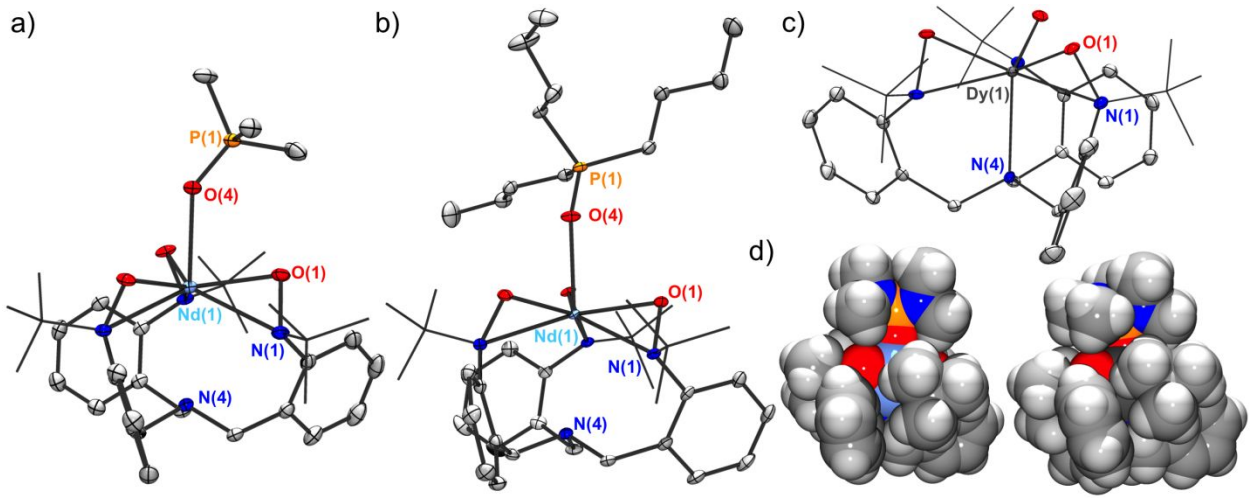

Figure 1. Thermal ellipsoid plots (50 % probability) of **2** (a), **5** (b), **9ø** (c) and space-fill models comparison of **8** (left) and **12** (right) (d).

With solid-state structures of neodymium adducts **2**-**8** and the previously reported $\mathbf{1}_{THF}$ in-hand, effects of the coordination of phosphoryl ligands were examined and compared with the solution-state dimerization constants p$K_{dimer\text{-}n}$ (**n** = **1**-**8**) (Figure 2).

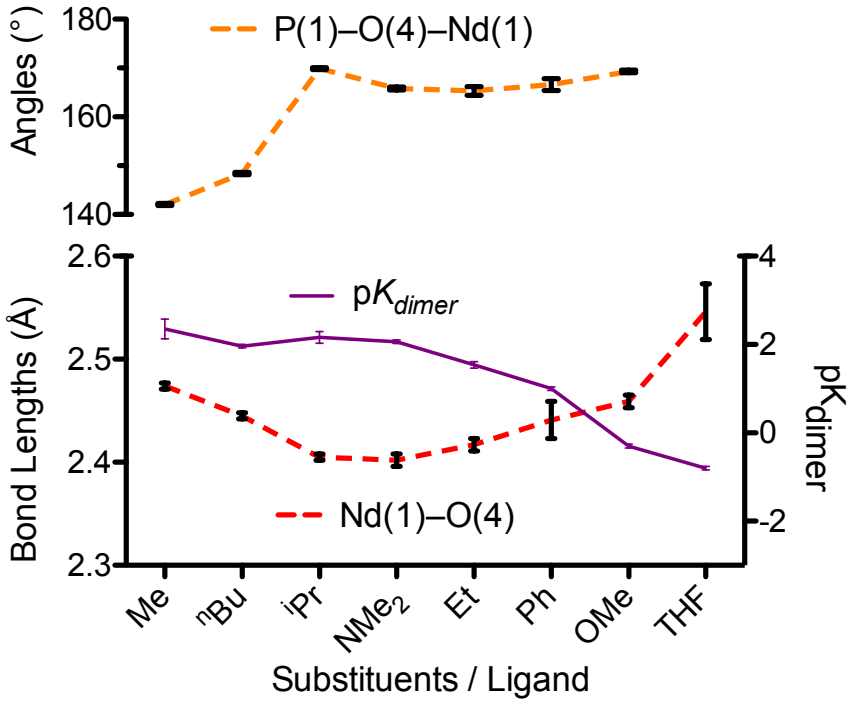

Figure 2. Bond lengths, angles, and pK_{dimer} comparison between neodymium complexes **2**-**8** and $\mathbf{1}_{THF}$ (d). Bond lengths and angles refer to the left axes,

pK_{dimer} values refer to the right axis. Connecting lines are provided only as a guide for the eye.

Coordination bonds Nd(1)-N_{NO} and Nd(1)-O_{NO} were statistically equivalent for compounds **2**-**8** (see Table S5 for key metrical parameters of complexes **2**-**12**) demonstrating similar equatorial coordination environments. Larger variability was observed for the apical coordination bonds Nd(1)-N(4) and Nd(1)-O(4), as well as the angle of coordination P(1)-O(4)-Nd(1) of the phosphoryl ligands. The latter parameter indicated two preferential coordination modes for the phosphoryl ligands: bent (**2** and **5**) or linear (**3**, **4**, **6**, **7** and **8**), as also observed in the Cambridge Structural Database (see Figure S53). Notably, complexes exhibiting a nearly linear coordination mode – which minimize the inter-ligand steric repulsion – demonstrated a positive correlation between the Nd(1)-O(4) bond lengths and the magnitude of their respective dimerization constants: weaker ligands relative to the monomerization process (larger K_{dimer}) were observed to possess longer Nd(1)-O(4) bonds.

A solid-state comparison between complexes **1**-**8** allowed us to draw a tentative qualitative correlation between key metric parameters (the Nd(1)-O(4)-P(1) angles and Nd(1)-O(4) bond distances) and solution-state dimerization constants. Having established the influence of different phosphoryl ligands of varying electronic and steric properties on [Nd(TriNOx)], the impact of a more Lewis acidic center, namely dysprosium, was examined (see Figure S40). As previously observed in the [(RE)TriNOx(THF)] series (RE = Y, La-Lu),[36] the lanthanide contraction results in the expected decrease in coordination bond lengths RE-N_{NO}, RE-O_{NO} and RE-O(4) with RE = Nd, Dy. Effects of the coordination of phosphoryl ligands and of the lanthanide contraction were also observed in the percent buried volume (%V_{bur}) of each complexes (Table 3).[44]

Table 3. Calculated %V_{bur} of complexes $\mathbf{1_{THF}}$, **4**, **7**, **8**, $\mathbf{9_{THF}}$, $\mathbf{9_{ø}}$, **10**, **11** and **12**

%V_{bur}	O=P(NMe_2)$_3$	O=P(^{i}Pr)$_3$	O=PEt_3	THF[35]	ø
Nd	78.7	78.2	78.3	79.9	/
Dy	80.3	79.6	79.4	81.3	87.0

In comparison with their THF analogues, both neodymium and dysprosium phosphoryl adducts exhibited a more open molecular aperture to accommodate

the shorter observed RE-O(4) bonds. Besides this, the closure of the molecular aperture upon the contraction is observed to be similar for any considered ancillary ligand. Finally, the $\%V_{bur}$ of the "naked" complex **9ø** was significantly higher in comparison with the previously reported THF-solvates where the highest $\%V_{bur}$ was obtained for the lutetium complex (82.6 %).[36] This effect is also highlighted by the Dy(1)-N(4) bond length in **9ø** which is the shortest observed for all RE complexes of the $TriNOx^{3-}$ framework (see Figures 1d and S41-S52 for space-fill views).

Thermogravimetric analyses. Bond length comparisons of neodymium (**1**-**8**) and dysprosium (**9**-**12**) complexes allowed for a deeper understanding of the coordination chemistry of the phosphoryl ligands. To gain more insight into the relative metal-phosphoryl ligands bond strengths, differential scanning calorimetry/thermogravimetric analyses (DSC/TGA, 10°C min^{-1}, N_2 flow) were conducted on complexes **2**-**8** and **10**-**11** (Figure 3 and S55-S64).

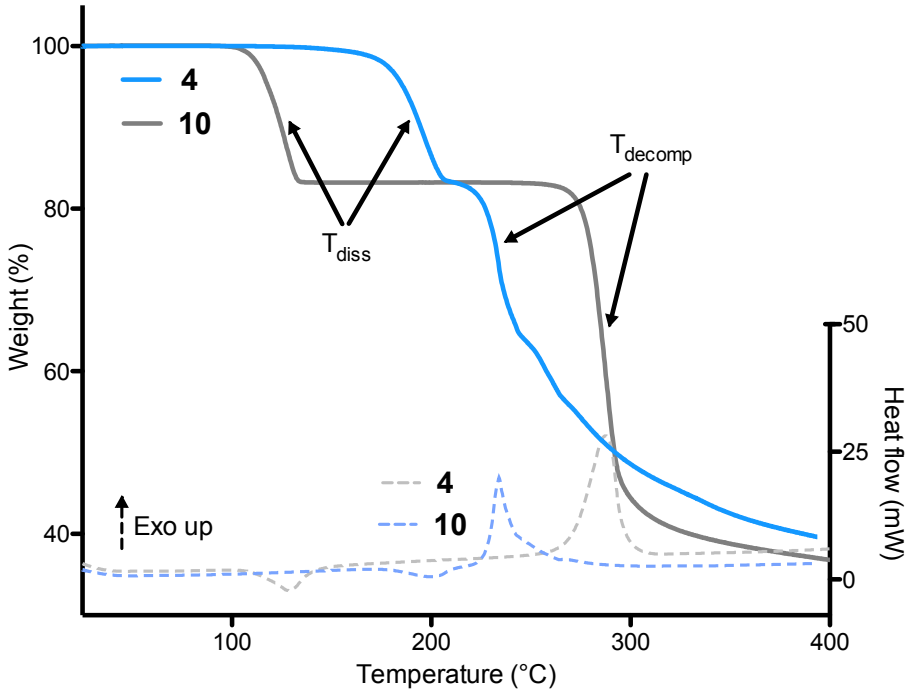

Figure 3. DSC (---, right axis) and TGA (–, left axis) thermographs of Nd (**4**) and Dy (**10**) adducts of $O{=}PEt_3$. T_{diss} and T_{decomp} were determined as the maxima of the first derivative of the TGA measurements (not depicted).

Table 4. Dissociation temperatures (T_{diss}) of phosphoryl ligands observed by DSC-TGA.

T_{diss} (°C)	$O{=}P(OMe)_3$	$O{=}PMe_3$	$O{=}PEt_3$	$O{=}P(^iPr)_3$	$O{=}P(NMe_2)_3$
Nd	152.0	181.0	196.2	217.4	211.8
Dy	/	/	126.2	134.1	152.5

All complexes depicted similar TGA profiles: an endothermic ancillary ligand dissociation (T_{diss}, except for **5** and **6**) followed by an exothermic decomposition of the $TriNOx^{3-}$ framework (T_{decomp}). Representative examples of the thermographs obtained for neodymium (**4**) and dysprosium (**10**) adducts of $O{=}PEt_3$ are presented in Figure 3. $TriNOx^{3-}$ decomposition was observed at about 234 °C for all neodymium complexes **2**–**8** while dysprosium adducts **10**–**12** experienced degradation around 283 °C (Figures S55–S64). This observation supports an increased Lewis acidity from Nd to Dy.[36] Converse to that expected trend, dissociations of ancillary phosphoryl ligands were observed at much lower temperatures (ΔT_{diss} = 59 to 83 °C, Table 4) for dysprosium complexes **10**–**12** than their respective neodymium congeners **4**, **7**, and **8**. This demonstrates a larger thermal stability for the coordinated phosphoryl ligands in Nd complexes than their Dy analogues.[45] Therefore, assuming similar lattice energies for pairs of complexes before and after the thermal dissociation of the phosphoryl ligands, and approximately identical rates of dissociation, the main contribution in ΔT_{diss} is the difference in the enthalpy of coordination $\Delta\Delta H_{coord}$ =

$\Delta H_{coord(Nd)} - \Delta H_{coord(Dy)}$, where $\Delta H_{coord(RE)}$ is the enthalpy of reaction associated with the formation of the RE-O=PR_3 coordination bonds. These observations establish a qualitative thermodynamic difference for the RE-O=PR_3 bond strengths between RE = Nd and RE = Dy. Recognizing the thermodynamic preferences of phosphoryl ligands for the [Nd(TriNOx)] fragment over their dysprosium congeners, the possibility of separating [Nd/Dy(TriNOx)] mixtures by leaching was next examined.

Separations experiments: neodymium/dysprosium. First, homogeneously dispersed equimolar solid-solutions of the two elements were synthesized and coordinated to the H_3TriNOx ligand (see SI). Two phosphoryl ligands were then targeted to optimize the separation conditions: trimethylphosphine oxide and tri(*n*-butyl)phosphine oxide. O=PMe_3 was observed to be the strongest ligand of the series while O=P(^{n}Bu)$_3$ afforded very large solubility to its adducts in alkane solvents. After an initial screening of solvents, diethyl ether (Et_2O) and *n*-hexane were selected for performing the leaching separation experiments using O=PMe_3 and O=P(^{n}Bu)$_3$, respectively. According to several metrics, simple

ethers, such as Et_2O, or linear alkanes (*n*-hexane, *n*-heptane) have been recognized as potential green organic solvents thanks to their low production and incineration costs.[46-47] An initial optimization of the separation conditions prompted us to design two different protocols: method A was employed for direct leaching experiments with $O{=}PMe_3$ in Et_2O; while method B (with $O{=}P(^nBu)_3$ in *n*-hexane) required an initial equilibration step in CH_2Cl_2 (Figure 4).

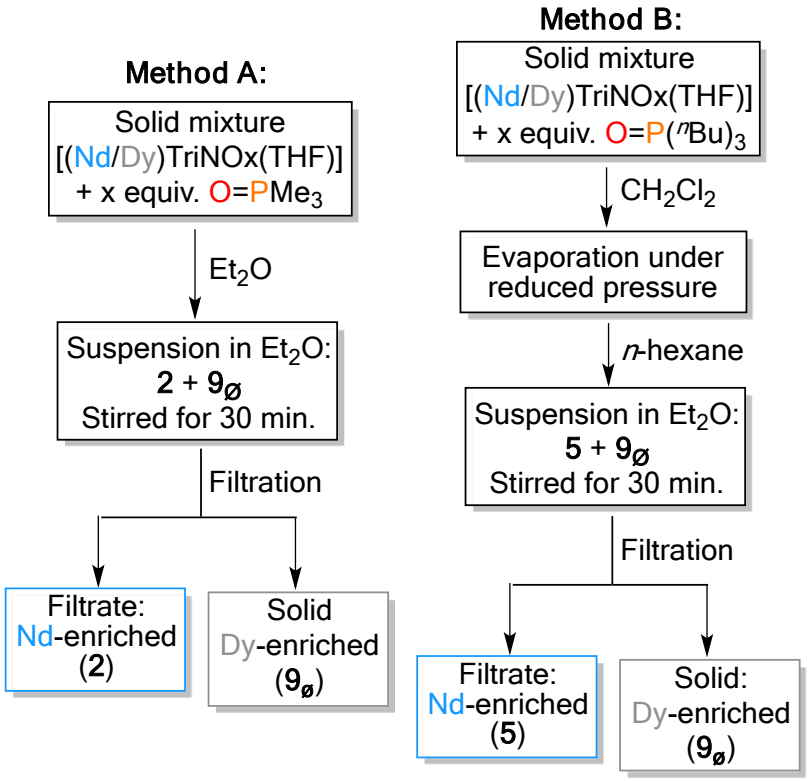

Figure 4. Schematic description of the separation experiments using $O=PMe_3$ (Method A) and $O=P(^{n}Bu)_3$ (Method B).

Compositions of each fraction (solid and filtrate) were determined by inductively coupled plasma-optical emission spectroscopy (ICP-OES) measurements. The purity of each portion was evaluated by the respective enrichment factors ($D_{Solid} = (n_{Dy}/n_{Nd})$; $D_{Filtrate} = (n_{Nd}/n_{Dy})$). The quality of the separation was estimated through the separation factor ($S_{Nd/Dy} = D_{Solid} \times D_{Filtrate}$). Following the optimization of experimental procedures, optimal volumes of solvent required for the leaching were also determined (Figures S65-S66) and kept constant for further experiments.

Finally, the influence of the amount of ancillary ligand was examined in duplicate; results for each method are reported on Figures 5 and 6.

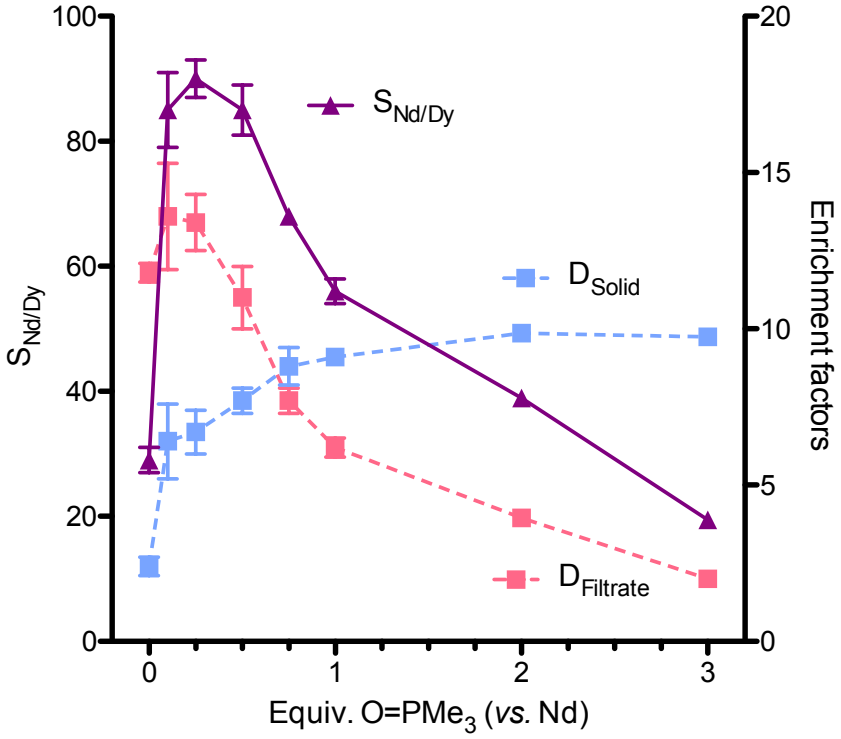

Figure 5. Impact of the amount of O=PMe$_3$ on the separation properties of method A. D_{Solid} and $D_{Filtrate}$ (---, right axis) and $S_{Nd/Dy}$ (–, left axis) were determined by ICP-OES (average of two independent runs).

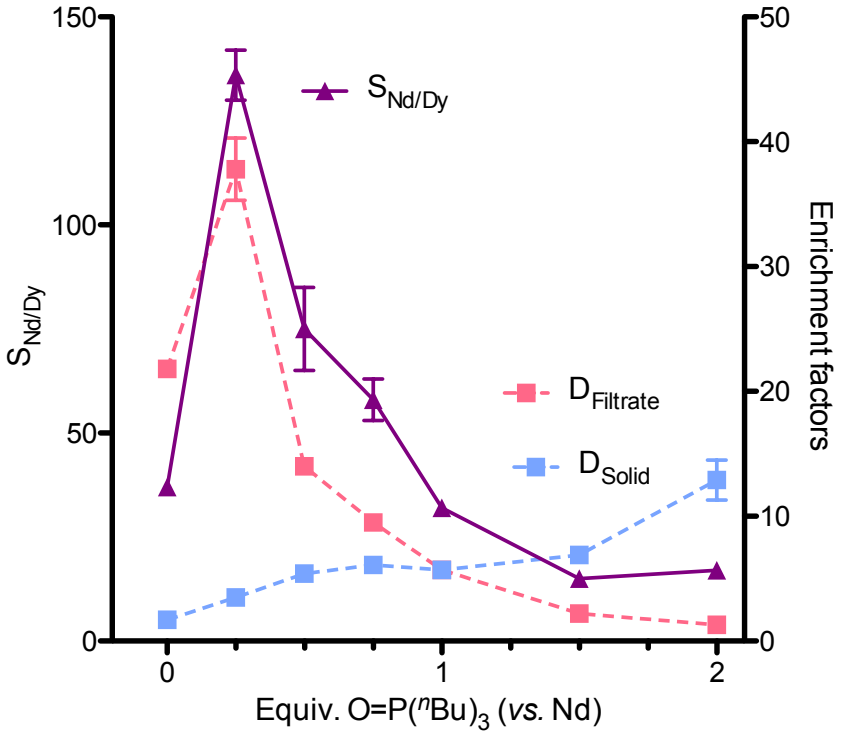

Figure 6. Impact of the amount of O=P(^{n}Bu)$_3$ on the separation properties of method B. D_{Solid} and $D_{Filtrate}$ (---, right axis) and $S_{Nd/Dy}$ (–, left axis) were determined by ICP-OES (average of two independent runs).

When 1 equivalent (molar equivalent *vs.* Nd) of phosphine oxide extractant was employed, both procedures demonstrated the expected thermodynamic preference and resulted in separation factors $S_{Nd/Dy}$ of 56±2 and 32±1 for method A and B respectively. Larger amount of extractants (> 1 equiv *vs.* Nd) resulted in a drop of the separation factor. This can be explained by an

increased coordination of the extractant to the [Dy(TriNOx)] fragments causing a decrease of the filtrate enrichment factor ($D_{Filtrate} \rightarrow 1$) which was not balanced by the increasing purity of the solid (D_{Solid} up to ~13). Sub-stoichiometric amounts of ancillary ligands resulted in an opposite effect: low amounts of extractant amplified the thermodynamic preference for neodymium, originating in high filtrate enrichment factors ($D_{Filtrate}$ = 13.4±0.9 and 37.8±2.5 for method A and B respectively, when 0.25 equiv. of phosphine oxides were employed). Conversely, the solid fractions were found to be relatively impure as a result of the lack of extractant. Despite these poorly enriched solids, the quality of the filtrate ($D_{Filtrate}$ = 37.8 is equivalent with **>** 97 % purity in Nd) resulted in appreciable separation factors of 90±3 and 136±6 for method A and B respectively (when 0.25 equiv. of extractant was used). Notably, mass balance was conserved through the separation and the recovery rates were generally good (Table S7-S8).

Separations experiments: lanthanum/neodymium. After confirming the ability of phosphoryl ligands to participate in neodymium/dysprosium separations, we

wondered if phosphoryl ligands could be employed for early/early rare earth separations. Such separations were not possible with our previous systems because of the dimeric nature of all early RE complexes (La-Eu).[35-37] Acknowledging the large solubility of O=P(^{n}Bu)$_3$ adduct **5** in *n*-hexane while all dimeric compounds $\mathbf{1_{dimer\text{-}HRE}}$ (HRE = La-Eu) proved to be mostly insoluble in alkane solvents, we targeted the separation of lanthanum and neodymium pairs as a proof of concept of this new strategy. We first examined the binding constant of O=P(^{n}Bu)$_3$ with [La(TriNOx)]$_2$ ($\mathbf{1_{dimer\text{-}La}}$), giving rise to a $K_{dimer\text{-}La}$ = 3.0 ± 0.1 x 10^{-2}. While small, the difference with $K_{dimer\text{-}5}$ (1.1 ± 0.1 x 10^{-2}) suggested the preferable coordination of O=P(^{n}Bu)$_3$ with [Nd(TriNOx)]$_2$ ($\mathbf{1_{dimer}}$). Separations experiments were conducted using a similar procedure as method B (Scheme 3, see SI for details). In this situation, the solid portion was enriched with $\mathbf{1_{dimer\text{-}La}}$, while the filtrate had an enhanced proportion of **5** (Scheme 3).

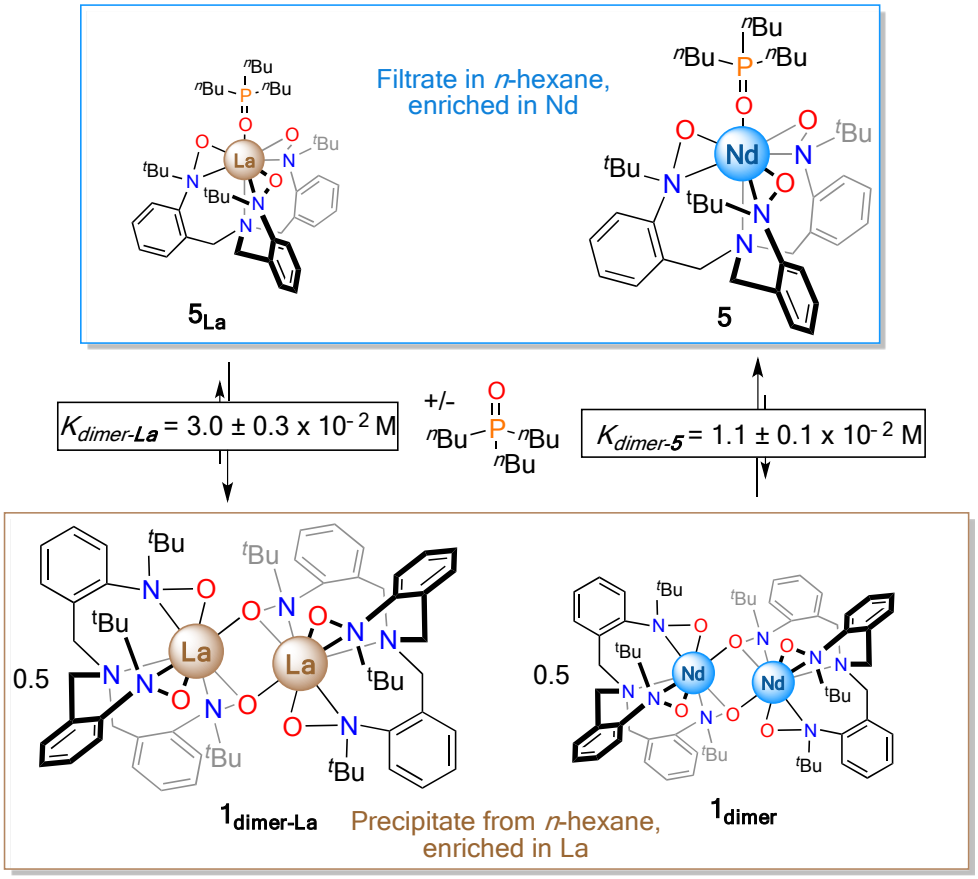

Scheme 3. Association equilibrium constants for $\mathbf{1}_{\text{dimer-La}}$ and $\mathbf{1}_{\text{dimer}}$.

As previously performed, we examined the influence of the amount of tri(*n*-butyl)phosphine oxide extractant on the separation performances (Figure 7). Control experiments in the absence of O=P(*n*Bu) demonstrated no level of separation. As expected and observed for Nd/Dy separations, increased amount of extractants led to improved solid purity (D_{Solid}) while decreasing the quality of the filtrate ($D_{Filtrate}$). Excessive amounts of O=P(*n*Bu) (2.5 equiv. *vs.* Nd) resulted

in unappreciable amounts of recovered solid, reducing the separation performance of the system. The overall best separations were observed for slight excess of extractant, with $S_{La/Nd}$ ~ 10. Although moderate, these results demonstrated the ability of the $TriNOx^{3-}$ system to separate pairs of early/early RE with the introduction of an external ligand.

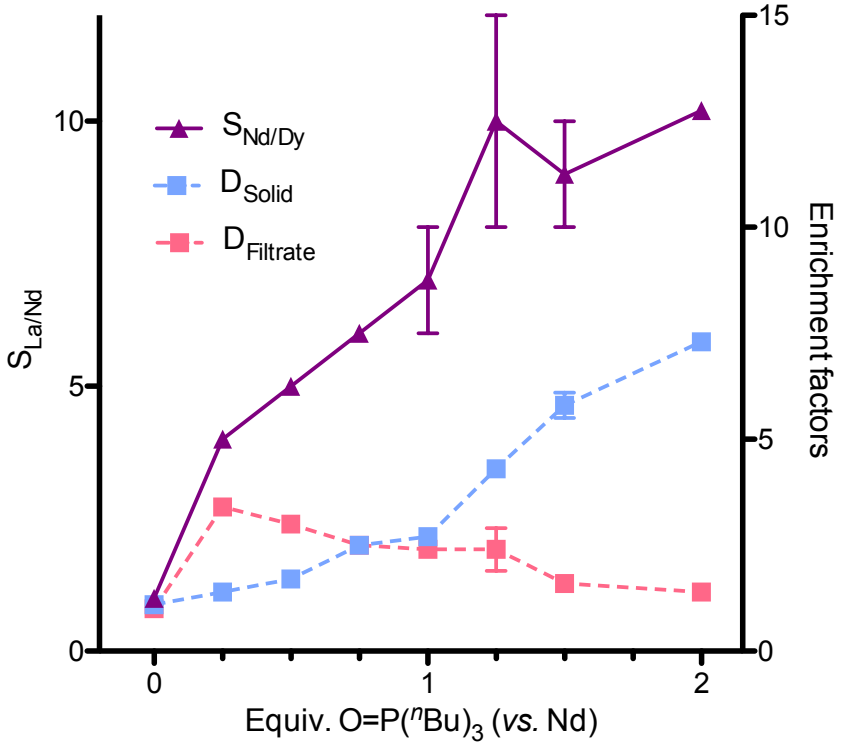

Figure 7. Impact of the amount of O=P(^{n}Bu)$_3$ on the separation properties of method B' for equimolar [(La/Nd)TriNOx] mixtures . D_{Solid} and $D_{Filtrate}$ (---, right

axis) and $S_{La/Nd}$ (–, left axis) were determined by ICP-OES (average of two independent runs).

Finally, THF solutions of oxalic acid (1.5 equiv) were added to isolated solid and filtrate portions. After drying, the resulting solid could be extracted first with *n*-hexane, releasing $O=P(^{n}Bu)_3$ in *ca.* 90 %. Further leaching with Et_2O allowed recovering H_3TriNOx (86 %) leaving RE-oxalates as the solid portion; confirming the recyclability of the separation system.

CONCLUSIONS

The binding of various phosphoryl ligands was examined with neodymium and dysprosium centers coordinated by the $TriNOx^{3-}$ ligand framework. Solution- and solid-state behaviors were investigated and allowed us to rationalize the coordination of ancillary ligands to the [RE(TriNOx)] system. As a result of the $TriNOx^{3-}$ properties and conversely to general trends, more Lewis acidic RE were observed to bind weakly to Lewis basic ancillary phosphoryl ligands. These findings were applied to the separation of Nd/Dy pairs with reasonable separation factors, while providing access to alternative leaching solvents. We

also demonstrated proof of concept for La/Nd separation, a combination inseparable with our original system. Hence, the use of ancillary ligands provided a more flexible approach for the separation of RE, compared to our previously reported system, based solely on self-association. In particular, solubilizing phosphoryl ligands allowed for greener leaching solvents. The separation results reported here were four to six times better than industrial solvent extraction systems based on mono-2-ethylhexylester(2-ethylhexyl)phosphinic acid (HEH(EHP)) or bis(2-ethylhexyl)phosphoric acid (HDEHP).[48] More generally, we demonstrated that understanding of the coordination chemistry of metal-extractant systems allows for improved separation results through leaching. In this way, connection of coordination chemistry to separations performance promises to reduce environmental impact by limiting the number of iterations required for metal separations. In the context of urban mining, the results presented here help to articulate design principles for new RE separations opportunities and improve understanding of synergistic effects in mixed extractant systems.[48]

Finally, the current work was limited to pairs of RE, however we believe that these findings could enable the separation of complex mixtures (**>** 2 RE), by incremental leaching steps. Work in this direction is currently underway in our laboratory.

EXPERIMENTAL SECTION

*Representative synthesis of **2***: $[NdTriNOx]_2$ (135 mg, 98 µmol) was suspended in CH_2Cl_2 (5 mL), $O{=}PMe_3$ (22.5 mg, 0.24 mmol, 2.5 equiv.) was dissolved in CH_2Cl_2 (2 mL). The two solutions were mixed and stirred for 1 hour to yield a clear blue solution. Volatiles were removed under reduce pressure. The solid was suspended in a mixture of Et_2O/hexanes (1:1, 5 mL). The suspension was filtered and washed with pentane (2×3 mL) to yield **2** as a pale blue solid (73 mg, 93 µmol, 48%) after drying. Single crystals suitable for X-ray analysis were grown by gas-diffusion of hexanes into a 1,2-difluorobenzene solution of the complex.

Syntheses of other complexes deviates from these conditions and are detailed in the Supporting Information. Crystallization conditions for all crystallographically characterized complexes are detailed in Table S2.

Representative separation experiment: Method A. In 20 mL scintillation vial, solid **[(Nd/Dy)(TriNOx)(THF)]** (80 mg) and $O{=}PMe_3$ (x equiv. *vs.* Nd, x ranges 0 to 3) were suspended in Et_2O (6 mL). The mixture was vigorously stirred for 30 minutes. The mixture was filtered over a pre-weighted medium-porosity fritted-glass filter and a pre-weighted filter flask, the vial was washed with Et_2O (2 mL) and the filter cake was washed a second time with Et_2O (2 mL). The solid (Dy-rich) and filtrate (Nd-rich) fractions were dried under vacuum and their respective masses were recorded. The Nd:Dy ratio were estimated by ^1H NMR in $CDCl_3$ and further measured by ICP-OES.

Full details of the separation experiments can be found in the Supporting Information.

ASSOCIATED CONTENT

Supporting Information. Synthetic and separation experiments details, spectroscopic, thermogravimetric, and crystallographic data (PDF).

AUTHOR INFORMATION

Corresponding Author

∗E-mail: schelter@sas.upenn.edu

ACKNOWLEDGMENT

The Camille and Henry Dreyfus Postdoctoral Program in Environmental Chemistry is greatly acknowledged for a fellowship to T.C. We thank Dr. Andrew R. McGhie (LRSM, UPenn) for insightful discussions on TGA data. This work is also supported by the U.S. Department of Energy, Office of Sciences, Office of Basic Sciences Separations and Analysis program under Award Number DE-SC0017259. We also acknowledge the Center for Actinide Science and Technology (CAST), an Energy Frontier Research Center (EFRC) funded by the U.S. Department of Energy, Office of Basic Energy Sciences (DE-SC0016568) for current support of T.C. The National Science Foundation Graduate Research Fellowship program is acknowledged for support to B.E.C.

REFERENCES

(1) IPCC *Climate Change 2014: Mitigation of Climate Change (WG III)*; IPCC: Geneva, Switzerland, 2014.

(2) Borges de Lima, I., Chapter 19 - Rare Earths Industry and Eco-management: A Critical Review of Recycling and Substitutes. In *Rare Earths Industry*, Elsevier: Boston, 2016; pp 293-304.
(3) Binnemans, K.; Jones, P. T.; Blanpain, B.; Van Gerven, T.; Yang, Y.; Walton, A.; Buchert, M. Recycling of rare earths: a critical review, *J. Cleaner Prod.* **2013**, *51*, 1-22, DOI 10.1016/j.jclepro.2012.12.037.
(4) Reck, B. K.; Graedel, T. E. Challenges in Metal Recycling, *Science* **2012**, *337*, 690-695, 10.1126/science.1217501.
(5) Marx, J.; Schreiber, A.; Zapp, P.; Walachowicz, F. Comparative Life Cycle Assessment of NdFeB Permanent Magnet Production from Different Rare Earth Deposits, *ACS Sustainable Chem. Eng.* **2018**, *6*, 5858-5867, DOI 10.1021/acssuschemeng.7b04165.
(6) Arshi, P. S.; Vahidi, E.; Zhao, F. Behind the Scenes of Clean Energy: The Environmental Footprint of Rare Earth Products, *ACS Sustainable Chem. Eng.* **2018**, *6*, 3311-3320, DOI 10.1021/acssuschemeng.7b03484.
(7) Lee, J. C. K.; Wen, Z. Rare Earths from Mines to Metals: Comparing Environmental Impacts from China's Main Production Pathways, *J. Ind. Ecol.* **2017**, *21*, 1277-1290, DOI 10.1111/jiec.12491.
(8) Rademaker, J. H.; Kleijn, R.; Yang, Y. Recycling as a Strategy against Rare Earth Element Criticality: A Systemic Evaluation of the Potential Yield of NdFeB Magnet Recycling, *Environ. Sci. Technol.* **2013**, *47*, 10129-10136, 10.1021/es305007w.
(9) Sprecher, B.; Xiao, Y.; Walton, A.; Speight, J.; Harris, R.; Kleijn, R.; Visser, G.; Kramer, G. J. Life Cycle Inventory of the Production of Rare Earths and the Subsequent Production of NdFeB Rare Earth Permanent Magnets, *Environ. Sci. Technol.* **2014**, *48*, 3951-3958, 10.1021/es404596q.
(10) Sprecher, B.; Kleijn, R.; Kramer, G. J. Recycling Potential of Neodymium: The Case of Computer Hard Disk Drives, *Environ. Sci. Technol.* **2014**, *48*, 9506-9513, DOI 10.1021/es501572z.
(11) Bandara, H. M. D.; Darcy, J. W.; Apelian, D.; Emmert, M. H. Value Analysis of Neodymium Content in Shredder Feed: Toward Enabling the

Feasibility of Rare Earth Magnet Recycling, *Environ. Sci. Technol.* **2014**, *48*, 6553-6560, DOI 10.1021/es405104k.

(12) Bandara, H. M. D.; Field, K. D.; Emmert, M. H. Rare earth recovery from end-of-life motors employing green chemistry design principles, *Green Chem.* **2016**, *18*, 753-759, 10.1039/C5GC01255D.

(13) Yang, Y.; Walton, A.; Sheridan, R.; Güth, K.; Gauß, R.; Gutfleisch, O.; Buchert, M.; Steenari, B.-M.; Van Gerven, T.; Jones, P. T.; Binnemans, K. REE Recovery from End-of-Life NdFeB Permanent Magnet Scrap: A Critical Review, *J. Sustain. Metall.* **2017**, *3*, 122-149, DOI 10.1007/s40831-016-0090-4.

(14) Jha, M. K.; Kumari, A.; Panda, R.; Rajesh Kumar, J.; Yoo, K.; Lee, J. Y. Review on hydrometallurgical recovery of rare earth metals, *Hydrometallurgy* **2016**, *165*, 2-26, DOI 10.1016/j.hydromet.2016.01.035.

(15) Sun, X.; Waters, K. E. Synergistic Effect between Bifunctional Ionic Liquids and a Molecular Extractant for Lanthanide Separation, *ACS Sustainable Chem. Eng.* **2014**, *2*, 2758-2764, 10.1021/sc500493d.

(16) Sun, X.; Waters, K. E. Development of Industrial Extractants into Functional Ionic Liquids for Environmentally Friendly Rare Earth Separation, *ACS Sustainable Chem. Eng.* **2014**, *2*, 1910-1917, 10.1021/sc500255n.

(17) Schaeffer, N.; Grimes, S.; Cheeseman, C. Interactions between trivalent rare earth oxides and mixed [Hbet][Tf2N]:H2O systems in the development of a one-step process for the separation of light from heavy rare earth elements, *Inorg. Chim. Acta* **2016**, *439*, 55-60, http://dx.doi.org/10.1016/j.ica.2015.09.015.

(18) Zhao, X.; Wong, M.; Mao, C.; Trieu, T. X.; Zhang, J.; Feng, P.; Bu, X. Size-Selective Crystallization of Homochiral Camphorate Metal-Organic Frameworks for Lanthanide Separation, *J. Am. Chem. Soc.* **2014**, *136*, 12572-12575, 10.1021/ja5067306.

(19) Ni, X.-L.; Xue, S.-F.; Tao, Z.; Zhu, Q.-J.; Lindoy, L. F.; Wei, G. Advances in the lanthanide metallosupramolecular chemistry of the cucurbit[n]urils, *Coord. Chem. Rev.* **2015**, *287*, 89-113, http://dx.doi.org/10.1016/j.ccr.2014.12.018.

(20) Yang, B.; Gao, Z.-Z.; Lu, J.-H.; Zhu, Q.-J.; Xue, S.-F.; Tao, Z.; Prior, T. J.; Redshaw, C.; Wei, G.; Xiao, X. Interaction of a symmetrical [small alpha],[small alpha][prime or minute],[small delta],[small delta][prime or minute]-tetramethyl-

cucurbit[6]uril with Ln3+: potential applications for isolation of lanthanides, *CrystEngComm* **2016**, *18*, 5028-5035, 10.1039/C6CE00134C.

(21) Tasaki-Handa, Y.; Abe, Y.; Ooi, K.; Narita, H.; Tanaka, M.; Wakisaka, A. Selective Crystallization of Phosphoester Coordination Polymer for the Separation of Neodymium and Dysprosium: A Thermodynamic Approach, *J. Phys. Chem. B* **2016**, *120*, 12730-12735, DOI 10.1021/acs.jpcb.6b09450.

(22) Van den Bogaert, B.; Havaux, D.; Binnemans, K.; Van Gerven, T. Photochemical recycling of europium from Eu/Y mixtures in red lamp phosphor waste streams, *Green Chem.* **2015**, *17*, 2180-2187, 10.1039/C4GC02140A.

(23) Van den Bogaert, B.; Gheeraert, L.; Leblebici, M. E.; Binnemans, K.; Van Gerven, T. Photochemical recovery of europium from non-aqueous solutions, *Phys. Chem. Chem. Phys.* **2016**, *18*, 29961-29968, 10.1039/C6CP06329B.

(24) Bonificio, W. D.; Clarke, D. R. Rare-Earth Separation Using Bacteria, *Environ. Sci. Technol. Lett.* **2016**, *3*, 180-184, 10.1021/acs.estlett.6b00064.

(25) Takahashi, Y.; Yamamoto, M.; Yamamoto, Y.; Tanaka, K. EXAFS study on the cause of enrichment of heavy REEs on bacterial cell surfaces, *Geochim. Cosmochim. Acta* **2010**, *74*, 5443-5462, http://dx.doi.org/10.1016/j.gca.2010.07.001.

(26) Park, D. M.; Reed, D. W.; Yung, M. C.; Eslamimanesh, A.; Lencka, M. M.; Anderko, A.; Fujita, Y.; Riman, R. E.; Navrotsky, A.; Jiao, Y. Bioadsorption of Rare Earth Elements through Cell Surface Display of Lanthanide Binding Tags, *Environ. Sci. Technol.* **2016**, *50*, 2735-2742, 10.1021/acs.est.5b06129.

(27) Roosen, J.; Binnemans, K. Adsorption and chromatographic separation of rare earths with EDTA- and DTPA-functionalized chitosan biopolymers, *J. Mater. Chem. A* **2014**, *2*, 1530-1540, 10.1039/C3TA14622G.

(28) Roosen, J.; Spooren, J.; Binnemans, K. Adsorption performance of functionalized chitosan-silica hybrid materials toward rare earths, *J. Mater. Chem. A* **2014**, *2*, 19415-19426, DOI 10.1039/C4TA04518A.

(29) Florek, J.; Chalifour, F.; Bilodeau, F.; Larivière, D.; Kleitz, F. Nanostructured Hybrid Materials for the Selective Recovery and Enrichment of Rare Earth Elements, *Adv. Funct. Mater.* **2014**, *24*, 2668-2676, 10.1002/adfm.201303602.

(30) Florek, J.; Giret, S.; Juere, E.; Lariviere, D.; Kleitz, F. Functionalization of mesoporous materials for lanthanide and actinide extraction, *Dalton Trans.* **2016**, *45*, 14832-14854, 10.1039/C6DT00474A.
(31) Zheng, X.; Liu, E.; Zhang, F.; Yan, Y.; Pan, J. Efficient adsorption and separation of dysprosium from NdFeB magnets in an acidic system by ion imprinted mesoporous silica sealed in a dialysis bag, *Green Chem.* **2016**, *18*, 5031-5040, 10.1039/C6GC01426G.
(32) Ling, L.; Wang, N.-H. L. Ligand-assisted elution chromatography for separation of lanthanides, *J. Chromatogr. A* **2015**, *1389*, 28-38, DOI 10.1016/j.chroma.2015.02.004.
(33) Willems, J. J. G.; Buschow, K. H. J. From permanent magnets to rechargeable hydride electrodes, *J. Less-Common Met.* **1987**, *129*, 13-30, DOI 10.1016/0022-5088(87)90029-4.
(34) Ying, T. K.; Gao, X. P.; Hu, W. K.; Wu, F.; Noréus, D. Studies on rechargeable NiMH batteries, *Int. J. Hydrogen Energy* **2006**, *31*, 525-530, DOI 10.1016/j.ijhydene.2005.04.018.
(35) Bogart, J. A.; Lippincott, C. A.; Carroll, P. J.; Schelter, E. J. An Operationally Simple Method for Separating the Rare-Earth Elements Neodymium and Dysprosium, *Angew. Chem. Int. Ed.* **2015**, *54*, 8222-8225, 10.1002/anie.201501659.
(36) Bogart, J. A.; Cole, B. E.; Boreen, M. A.; Lippincott, C. A.; Manor, B. C.; Carroll, P. J.; Schelter, E. J. Accomplishing simple, solubility-based separations of rare earth elements with complexes bearing size-sensitive molecular apertures, *Proc. Natl. Acad. Sci. U.S.A.* **2016**, *113*, 14887-14892, 10.1073/pnas.1612628113.
(37) Cole, B. E.; Falcones, I. B.; Cheisson, T.; Manor, B.; Carroll, P.; Schelter, E. J. A Molecular Basis to Rare Earth Separations for Recycling: Tuning TriNOx Ligand Properties for Improved Performance, *Chem. Commun.* **2018**, *54*, 10276–10279, DOI 10.1039/C8CC04409K.
(38) Fang, H.; Cole, B. E.; Qiao, Y.; Bogart, J. A.; Cheisson, T.; Manor, B. C.; Carroll, P. J.; Schelter, E. J. Electro-kinetic Separation of Rare Earth Elements

Using a Redox-Active Ligand, *Angew. Chem. Int. Ed.* **2017**, *56*, 13450-13454, DOI 10.1002/anie.201706894.

(39) Platt, A. W. G. Lanthanide phosphine oxide complexes, *Coord. Chem. Rev.* **2017**, *340*, 62-78, DOI 10.1016/j.ccr.2016.09.012.

(40) Donoghue, J. T.; Peters, D. A. Coordination chemistry of phosphoryl compounds – I, *J. Inorg. Nucl. Chem.* **1969**, *31*, 467-470, DOI 10.1016/0022-1902(69)80490-2.

(41) Choquette, K. A.; Sadasivam, D. V.; Flowers, R. A. Uncovering the Mechanistic Role of HMPA in the Samarium Barbier Reaction, *J. Am. Chem. Soc.* **2010**, *132*, 17396-17398, DOI 10.1021/ja1088925.

(42) Sues, P. E.; Lough, A. J.; Morris, R. H. Synthesis, Characterization, and Activity of Yttrium(III) Nitrate Complexes Bearing Tripodal Phosphine Oxide and Mixed Phosphine-Phosphine Oxide Ligands, *Inorg. Chem.* **2012**, *51*, 9322-9332, DOI 10.1021/ic3010147.

(43) Laurence, C.; Gal, J.-F., *Lewis Basicity and Affinity Scales: Data and Measurement*. John Wiley & Sons, Ltd: 2009.

(44) Falivene, L.; Credendino, R.; Poater, A.; Petta, A.; Serra, L.; Oliva, R.; Scarano, V.; Cavallo, L. SambVca 2. A Web Tool for Analyzing Catalytic Pockets with Topographic Steric Maps, *Organometallics* **2016**, *35*, 2286-2293, DOI 10.1021/acs.organomet.6b00371.

(45) Donia, A. M. Thermal stability of transition-metal complexes, *Thermochim. Acta* **1998**, *320*, 187-199, DOI 10.1016/S0040-6031(98)00472-9.

(46) Jessop, P. G. Searching for green solvents, *Green Chem.* **2011**, *13*, 1391-1398, 10.1039/C0GC00797H.

(47) Capello, C.; Fischer, U.; Hungerbuhler, K. What is a green solvent? A comprehensive framework for the environmental assessment of solvents, *Green Chem.* **2007**, *9*, 927-934, 10.1039/B617536H.

(48) Krishnamurthy, N.; Gupta, C. K., *Extractive Metallurgy of Rare Earths*. CRC Press: 2016.

SYNOPSIS. Incorporation of ancillary phosphoryl ligands into a rare-earth (RE) separation system increased the system's scope and sustainability aspects.

TABLE OF CONTENTS GRAPHIC.